LQR/PID Controller Design of PLC-based Inverted Pendulum

Kaset Sirisantisamrid, Napasool Wongvanich*, Suphan Gulpanich, and Narin Tammarugwattana

***Abstract*—This paper presents an LQR based PID controller to control the inverted pendulum system. The control design employs a control zoning approach whereby the entire pendulum system is divided into two regions: a normal pendulum region and the inverted pendulum region where the system is approximately linear close to the upright position. The LQR architecture is used to obtain optimal gains for the PID controller. An algebraic approach is also presented for selection of Q and R matrices. Experimental implementations with a PLC based system show that the computed gains yield the most stable controlled responses compared to the gains chosen through trial and errors.**

***Index Terms*—LQR control, PID control, PLC, Inverted Pendulum**

I. Introduction

THE classical Proportional Integral Derivative (PID) controller has remained the most popular industrial controller over the last six decades, despite the enormous hosts of development over the same period [1]. Various PID tuning methods have been developed by a number of researchers in the last 40 years. Developments in evolutionary algorithms and particle swarm optimization have led to the application of these methods for PID tuning [2], [3]. Other PID tuning approaches include the direct search algorithms and online optimization based approaches [4], [5]. Although these methods have resulted in the automatic tuning of the PID controllers, they require significant computational loading, and are not suitable for real time applications.

The Inverted Pendulum system is an inherently unstable system which is coupled with highly nonlinear dynamics. This feature alone makes the inverted pendulum system a challenging one, and also making it a primitive benchmark for comparing the various control approaches. Several advanced control designs have been presented, including fuzzy logics [6], [7]. These approaches however, require large training sets, and for the case of fuzzy based designs, a large set of rules which further complicates the control for higher order systems.

The Linear Quadratic Regulator (LQR) is well known in modern control, and besides the PID has been widely used. The LQR is used to obtain maximal performance of the system by minimizing the cost function relating the states and the control input. Through the use of optimal control theory, LQR is reduced to the solving of Algebraic Riccati Equation (ARE) to obtain the transformation matrix $\mathbf{P}$. The weight matrices $\mathbf{Q}$ and $\mathbf{R}$ are usually obtained through trial-and-error and thus sub-optimal. Bryson [8] developed the iterative tuning algorithm for selecting $\mathbf{Q}$ and $\mathbf{R}$. Kumar [9] developed an algebraic method of selecting the $\mathbf{Q}$ and $\mathbf{R}$ matrices for a 3×3 system. This work extends this method to a 5×5 system for the application of controlling the nonlinear inverted pendulum system. Furthermore, to ensure simplicity of the controller designs, a control-zoning approach is also employed.

Manuscript received December 05, 2017; revised January 23, 2018

Kaset Sirisantisamrid, Napasool Wongvanich, Suphan Gulpanich and Narin Tammarugwattana are with the Department of Instrumentation and Control Engineering, Faculty of Engineering, King Mongkut's Institute of Technology Ladkrabang, Bangkok, Thailand. E-mail: (kaset.si@kmitl.ac.th,napasool.wo@kmitl.ac.th,suphan.gu@kmitl.ac.th, narin.ta@kmitl.ac.th).

* Corresponding author

II. Methodology

A. The LQR controller outline

Consider the following linear-time invariant system described in the state-space form defined:

$$\dot{\mathbf{x}} = \mathbf{A}\mathbf{x} + \mathbf{b}u \tag{1a}$$

$$\mathbf{y} = \mathbf{C}\mathbf{x} \tag{1b}$$

$$\mathbf{x} \equiv [x_1, x_2, \ldots, x_n]^T, \mathbf{x_0} \equiv \left[x_{10}, \ldots, x_{n0}\right]^T \tag{1c}$$

where $x_i = x_i(t)$, i=1,...,n is a quantity of state i at time t (s), $\mathbf{x}$ is the $n \times 1$ state vector, $\mathbf{x_0}$ is the initial state vector, $\mathbf{y}$ is the measurement state vector, $\mathbf{u}$ is the input. The main assumption here is that the input u is time-dependent only, and does not depend on $\mathbf{x}_0$. The conventional Linear Quadratic Regulator (LQR) control seeks an optimal controller u_{opt} that minimizes the cost function:

$$J = \int_0^\infty \mathbf{x}^T\mathbf{Q}\mathbf{x} + \mathbf{u}^T\mathbf{R}\mathbf{u}\, dt \tag{2}$$

where $\mathbf{Q} = \mathbf{Q}^T$ is a positive semidefinite matrix, and $\mathbf{R}$ is a positive definite matrix. Matrix $\mathbf{Q}$ is the matrix penalizing the deviation of the states from the equilibrium, while matrix $\mathbf{R}$ is the matrix penalizing the control input size.

Through the use of optimal control theory, the optimal gain vector $\mathbf{K}$ is given by:

$$\mathbf{K} = \mathbf{R}^{-1}\mathbf{B}^\mathbf{T}\mathbf{P} \tag{3}$$

where matrix $\mathbf{P}(n\times n)$ is the solution of the algebraic Riccati Equation defined:

$$\mathbf{A}^T\mathbf{P} + \mathbf{P}\mathbf{A} + \mathbf{Q} - \mathbf{P}\mathbf{B}\mathbf{R}^{-1}\mathbf{B}^T\mathbf{P} = 0 \tag{4}$$

The selection of matrices $\mathbf{Q}$ and $\mathbf{R}$ have great bearings on the resulting controller being designed. If these matrices are simply chosen as simple diagonal matrices, the quadratic performance index of Equation (2) is thus the weighted integrals of the squared errors of the states and inputs. In practice these matrices are usually chosen arbitrarily first, then undergo manual tuning by trial and errors to achieve the required response. To save time and thus avoid this scenario, the following section gives an algebraic procedure for solving for these matrices explicitly for a fifth order system.

ISBN: 978-988-14047-8-7
ISSN: 2078-0958 (Print); ISSN: 2078-0966 (Online)

B. Algebraic method for selecting the $\mathbf{Q}$ *and* $\mathbf{R}$ *matrices*

Consider a specific fifth order state space system with the following state matrices:

$$\mathbf{A} = \begin{bmatrix} 0 & 1 & 0 & 0 & 0 \\ 0 & a_{22} & 0 & a_{24} & 0 \\ 0 & 0 & 0 & 1 & 0 \\ 0 & 0 & 0 & 0 & 1 \\ 0 & a_{52} & 0 & a_{54} & 0 \end{bmatrix}, \mathbf{B} = \begin{bmatrix} 0, b_2, 0, 0, b_5 \end{bmatrix}^T \quad (5a)$$

$$\mathbf{C} = \begin{bmatrix} c_1, \ldots, c_5 \end{bmatrix} \quad (5b)$$

This state space representation is typical for optimal tuning designs of PID controllers using the LQR theory. The procedure of LQR controller design requires the minimization of the cost function J of Equation (2). The state feedback control law that minimizes J is:

$$\mathbf{u} = -\mathbf{K}\mathbf{x} \quad (6)$$

where the optimal gain vector $\mathbf{K}$ is given by Equation (3).

Suppose that the weight matrices $\mathbf{Q}$ and $\mathbf{R}$, as well as the transformation matrix $\mathbf{P}$ are chosen as defined:

$$\mathbf{Q} = \begin{bmatrix} q_1 & & & & \\ & q_2 & & & \\ & & q_3 & & \\ & & & q_4 & \\ & & & & q_5 \end{bmatrix}, \mathbf{P} = \begin{bmatrix} p_{11} & p_{12} & \cdots & p_{15} \\ p_{21} & p_{22} & \cdots & p_{25} \\ \cdots & \cdots & \cdots & \cdots \\ p_{51} & p_{52} & \cdots & p_{55} \end{bmatrix} \quad (7)$$

$$\mathbf{R} = r \quad (8)$$

where r is an arbitrarily chosen scalar. Consider now the closed loop state equation defined:

$$\dot{\mathbf{x}}_c = (\mathbf{A} - \mathbf{B}\mathbf{K})\,\mathbf{x_c} \quad (9)$$

where $\mathbf{x}_c$ is the closed loop state. For stability the eigenvalues of the closed loop state transition matrix $\mathbf{A} - \mathbf{B}\mathbf{K}$ should all be negative, in other words, all lie on the left hand plane in a pole-zero diagram. The characteristic equation of the closed loop state transition matrix is:

$$f(s) = p_1 s + p_2 s^2 + p_3 s^3 + p_4 s^4 + s^5 = 0 \quad (10)$$

where:

$$p_1 = \frac{a_{22}b_2b_5p_{23} + a_{22}b_5^2p_{35} - a_{24}b_2b_5p_{12} - a_{24}b_5^2p_{15}}{r} \frac{-a_{52}b_2^2p_{23} - a_{52}b_2b_5p_{35} + a_{54}b_2^2p_{12} + a_{54}b_2b_5p_{15}}{r} \quad (11a)$$

$$p_2 = \frac{-a_{22}b_2b_5p_{24} - a_{22}b_5^2p_{45} + a_{24}b_2b_5p_{22} + a_{24}b_5^2p_{25} + a_{52}b_2^2p_{24}}{r} \frac{a_{52}b_2b_5p_{45} - a_{54}b_2^2p_{22} - a_{54}b_2b_5p_{25}}{r} \frac{+a_{22}a_{54}r - a_{24}a_{52}r + b_2b_5p_{23} + b_5^2p_{35}}{r} \quad (11b)$$

$$p_3 = -\frac{a_{22}b_2b_5p_{25} - a_{22}b_5^2p_{55} - b_2^2a_{52}p_{25} - a_{52}b_2b_5p_{55} - b_2^2p_{12}}{r} \frac{-b_2b_5p_{15} - b_2b_5p_{24} - b_5^2p_{45} + a_{54}r}{r} \quad (11c)$$

$$p_4 = -\frac{-b_2^2p_{22} - 2b_2b_5p_{25} - b_5^2p_{55} + a_{22}r}{r} \quad (11d)$$

The desired characteristics of the fifth order system, for a given ξ and ω_n, can be written:

$$\begin{aligned} f_{desired}(s) &= s(s + \xi\omega_n)^2(s^2 + 2\xi\omega_n + \omega_n)^2 \\ &= s^5 + 4\xi\omega_n s^4 + \omega_n^2(5\xi^2 + 1)s^3 \\ &\quad + 2\omega_n^3\xi(\xi^2 + 1)s^2 + \omega_n^4\xi^2 s \end{aligned} \quad (12)$$

Equating the co-efficients of Equation (12) to Equations (11a) - (11d), and assuming that p_{12}, p_{13}, p_{15}, p_{24}, p_{25}, p_{45} and p_{55} are known, yields a system of three equations in three unknowns, which is solved in Maple to yield the values for p_{22}, p_{23} and p_{35}:

$$\begin{aligned} p_{22} = \tfrac{1}{b_2^2(-a_{22}b_5 + a_{52}b_2)} \Big(&(-a_{22}p_{55} + 2p_{45})b_5^3 \\ &+ 2(\tfrac{1}{2}p_{55}a_{52} + p_{24} + p_{15})b_2b_5^2 + (2b_2^2p_{12} \\ &- 10r(\tfrac{1}{10}a_{22}^2 + \tfrac{2}{5}\omega_n\xi a_2 2 + (\xi^2 + \tfrac{1}{5})\omega_n^2 + \tfrac{1}{5}a_{54}))b_5 \\ &+ 4a_{52}r(\xi\omega_n + \tfrac{1}{4}a_{22})b_2 \Big) \end{aligned} \quad (13a)$$

$$\begin{aligned} p_{23} = \tfrac{1}{b_2^2(-a_{22}b_5 + a_{52}b_2)} \Big(&- a_{24}b_5^4p_{45} - (p_{45}a_{22}^2 - p_{35}a_{22} \\ &+ (p_{15} + p_{24})a_{24} - p_{45}a_{54})b_2b_5^3 + ((-p_{24}a_{22}^2 \\ &+ 2p_{45}a_{52}a_{22} - p_{12}a_{24} - p_{35}a_{52} + a_{54}(p_{15} \\ &+ p_{24}))b_2^2 + 5a_{24}r((\xi^2 + \tfrac{1}{5})\omega^2 + \tfrac{4}{5}\omega\xi a_{22} \\ &+ \tfrac{1}{5}a_{22}^2 + \tfrac{1}{5}a_{54}))b_5^2 - (2((-p_{24}a_{22}a_{52} + \tfrac{1}{2}p_{45}a_{52}^2 \\ &- \tfrac{1}{2}a_{54}p_{12})b_2^2 + (\xi a_{22}(\xi^2 + 1)\omega^3 + a_{54}(\tfrac{5}{2}\xi^2 + \tfrac{1}{2})\omega^2 \\ &+ 2\xi(a_{22}a_{54} + a_{24}a_{52})\omega + a_{22}a_{24}a_{52} + \tfrac{1}{2}a_{54}^2)r))b_2b_5 \\ &+ 2(-\tfrac{1}{2}p_{24}b_2^2a_{52} + ((\xi^3 + \xi)\omega^3 + 2\omega\xi a_{54} \\ &+ \tfrac{1}{2}a_{24}a_{52})r)a_{52}b_2^2 \Big) \end{aligned} \quad (13b)$$

$$\begin{aligned} p_{35} = \tfrac{1}{b_2^2(-a_{22}b_5 + a_{52}b_2)} \Big(&- b_2^2p_{12} - b_5(a_{52}p_{55} \\ &+ p_{15} + p_{24})b_2 + (a_{22}p_{55} - p_{45})b_5^2 + 5r((\xi^2 \\ &+ \tfrac{1}{5})\omega^2 + \tfrac{1}{5}a_{54}) \Big) \end{aligned} \quad (13c)$$

Consider now the element-wise form of the algebraic Riccati Equation:

$$\begin{aligned} &\begin{bmatrix} 0 & 0 & 0 & 0 & 0 \\ 1 & a_{22} & 0 & 0 & a_{52} \\ 0 & 0 & 0 & 0 & 0 \\ 0 & a_{24} & 1 & 0 & a_{54} \\ 0 & 0 & 0 & 1 & 0 \end{bmatrix} \begin{bmatrix} p_{11} & p_{12} & \cdots & p_{15} \\ p_{21} & p_{22} & \cdots & p_{25} \\ \cdots & \cdots & \cdots & \cdots \\ p_{51} & p_{52} & \cdots & p_{55} \end{bmatrix} \\ &+ \begin{bmatrix} p_{11} & p_{12} & \cdots & p_{15} \\ p_{21} & p_{22} & \cdots & p_{25} \\ \cdots & \cdots & \cdots & \cdots \\ p_{51} & p_{52} & \cdots & p_{55} \end{bmatrix} \begin{bmatrix} 0 & 1 & 0 & 0 & 0 \\ 0 & a_{22} & 0 & a_{24} & 0 \\ 0 & 0 & 0 & 1 & 0 \\ 0 & 0 & 0 & 0 & 1 \\ 0 & a_{52} & 0 & a_{54} & 0 \end{bmatrix} \\ &+ \begin{bmatrix} q_1 & & & & \\ & q_2 & & & \\ & & q_3 & & \\ & & & q_4 & \\ & & & & q_5 \end{bmatrix} - \frac{1}{r} \begin{bmatrix} p_{11} & p_{12} & \cdots & p_{15} \\ p_{21} & p_{22} & \cdots & p_{25} \\ \cdots & \cdots & \cdots & \cdots \\ p_{51} & p_{52} & \cdots & p_{55} \end{bmatrix} \\ &\times \begin{bmatrix} 0, b_2, 0, 0, b_5 \end{bmatrix}^T \begin{bmatrix} 0, b_2, 0, 0, b_5 \end{bmatrix} \\ &\times \begin{bmatrix} p_{11} & p_{12} & \cdots & p_{15} \\ p_{21} & p_{22} & \cdots & p_{25} \\ \cdots & \cdots & \cdots & \cdots \\ p_{51} & p_{52} & \cdots & p_{55} \end{bmatrix} = \mathbf{0} \end{aligned} \quad (14)$$

Note that since the weight matrix $\mathbf{Q}$ of Equation (7) is chosen to be a diagonal matrix, only the diagonals of the matrix Equation (14) are considered to simplify computations. This simplification yields five equations in five unknowns which

is readily solved for the elements $q_1, \ldots, q_5$ in Maple:

$$q_1 = \frac{b_2 p_{12} + b_5 p_{15}^2}{r} \tag{15a}$$

$$q_2 = \frac{1}{r}\left(-2a_{22}p_{22} - 2a_{52}p_{25} - 2p_{12}\right)r + \left(b_2 p_{22} + b_5 p_{25}\right)^2 \tag{15b}$$

$$q_3 = \frac{b_2 p_{23} + b_5 p_{35}^2}{r} \tag{15c}$$

$$q_4 = \frac{(-2a_{24}p_{24} - 2a_{54}p_{45} - 2p_{34})r + (b_2 p_{24} + b_5 p_{45})^2)}{r} \tag{15d}$$

$$q_5 = \frac{b_2^2 p_{25}^2 + 2b_2 b_5 p_{25} p_{55} + b_5^2 p_{55}^2 - 2p_{45}r)}{r} \tag{15e}$$

The optimal gain K_{opt} of Equation (3), in element wise form, is now:

$$\mathbf{K} = \left[\frac{b_2 p_{12} + b_5 p_{15}}{r}, \frac{b_2 p_{22} + b_5 p_{25}}{r}, \frac{b_2 p_{23} + b_5 p_{35}}{r}, \frac{b_2 p_{24} + b_5 p_{45}}{r}, \frac{b_2 p_{25} + b_5 p_{55}}{r},\right]^T \tag{16}$$

where the elements are computed by substituting Equations (13a) - (13c) into Equation (16).

III. Results and Discussion

A. The Inverted Pendulum system setup

The setup of the inverted pendulum on a cart is shown in Figure 1. The cart can move back and forth along a support rail. The cart also has two wires, one is connected to the servo driver (R88D-KP01H), which is in turn connected to a PLC of Sysmac C-series CP1H 40 I/O model. The other wire is connected to the encoder which is for feedback of the cart position and velocity. The PLC sends out high frequency pulse signals to command the position controller of servo to achieve the required cart position and velocity. The system is connected to CX programmer for access and changing the controller gains via the `PID(190)` command of the PLC. A PLC datalogging system is also used for data acquisition and for viewing the control signals. Figure 2 shows the interaction between the PLC and the servo motors. All data are saved in a `.txt` file, and can be viewed in MATLAB.

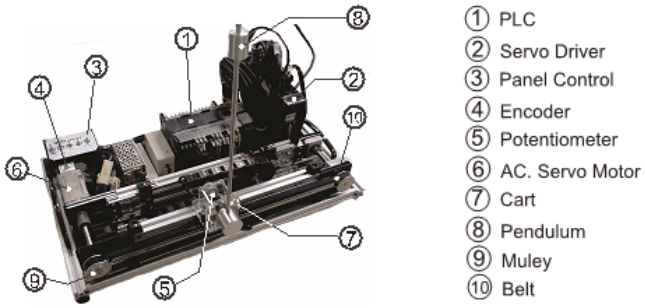

Fig. 1. The inverted pendulum on a cart

B. The Inverted Pendulum Model

Consider an inverted pendulum suspended on a moving cart as shown in Figure 3:

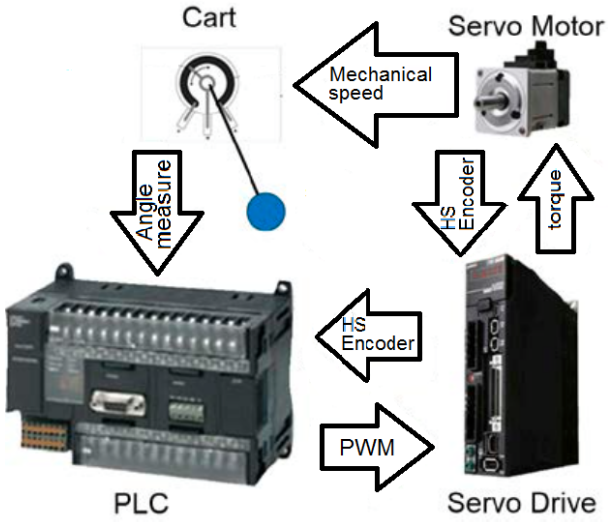

Fig. 2. The interaction between the PLC and the servo motors for the inverted pendulum system

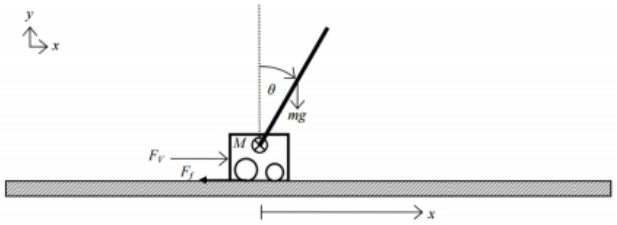

Fig. 3. The inverted pendulum on a cart

The differential equations governing the motion of the inverted pendulum are defined:

$$(M+m)\ddot{x} + \gamma_2 \dot{x} = F_v + ml\sin\theta\,(\dot{\theta})^2 - ml\cos\theta\,\ddot{\theta} \tag{17a}$$

$$(I + ml^2)\,\ddot{\theta} = mgl\sin\theta - mgl\cos\theta\,\ddot{x} \tag{17b}$$

where M and m are the masses of the cart and pendulum respectively (kg), l the pendulum length (m), g the gravitational constant (m s^{-2}), β_1 the damping constant of the cart (kg m s^{-1}), F_v the applied force onto the cart, x the cart position and θ the pendulum angle. Equations (17a) and (17b) can be linearized to yield the following differential equations:

$$\ddot{x} = -\frac{mg}{M}\theta - \frac{\gamma_2}{M}\dot{x} + \frac{\gamma_1}{M}V \tag{18}$$

$$\ddot{\theta} = \frac{(M+m)g}{ml}\theta - \frac{\gamma_2}{Ml}\dot{x} - \frac{\gamma_1}{Ml}V \tag{19}$$

Equations (18) and (19) can be expressed as state space equations where the state matrices are:

$$\mathbf{A} = \begin{bmatrix} 0 & 0 & 1 & 0 \\ 0 & 0 & 0 & 1 \\ 0 & -\frac{mg}{M} & -\frac{\gamma_2}{M} & 0 \\ 0 & \frac{(M+m)g}{ml} & -\frac{\gamma_2}{Ml} & 0 \end{bmatrix}, \quad \mathbf{B} = \begin{bmatrix} 0 \\ 0 \\ \frac{\gamma_1}{M} \\ \frac{-\gamma_1}{Ml} \end{bmatrix} \tag{20}$$

C. The Inverted Pendulum Control: Defining the control regions

Equation (20) gives the linearized dynamical model equation of the inverted pendulum that assumes the value of θ is small so that $\dot{\theta}$ =0. However, this assumption is generally not true for most operating regions of the inverted pendulum,

ISBN: 978-988-14047-8-7
ISSN: 2078-0958 (Print); ISSN: 2078-0966 (Online)

and thus designing a controller on the linearized dynamical model itself would likely result in a sub-optimal design. To achieve optimal design the entire system is thus divided into two regions in which the reference angle θ=0 is taken from the upright position: the normal pendulum region and the inverted pendulum region, where the normal pendulum region is between -45° $\leq \theta \leq$ 45° and the inverted pendulum region is between 45° $< \theta <$ -45° as shown in Figure 4. This division is similar to the control zoning approaches used in many industrial PLCs in level and temperature controls. For future references the inverted pendulum region will also be termed the linear region. Figure 5 shows the flowchart describing the implementation of the inverted pendulum control through a PLC. It is seen that the pendulum regions defined in Figure 4 is specified into the PLC system.

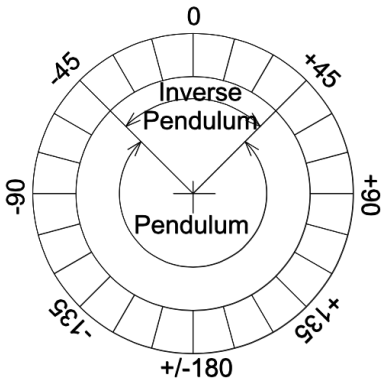

Fig. 4. Defining the pendulum regions with $\theta = 0°$ as reference

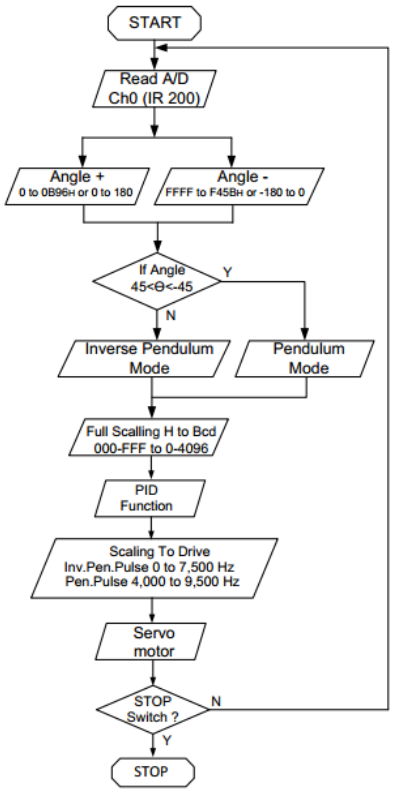

Fig. 5. The PLC based inverted pendulum system flowchart

D. Controlling the inverted pendulum in the normal pendulum region

In controlling the inverted pendulum setup in the normal pendulum region, a simple PID controller is used to allow implementation onto the PLC. In this region the proportional gain K_p is set to be large while the integral time T_i is set small, to allow maximum increase of the cart speed in order to generate sufficient forces to swing the pendulum. The minimal T_i value is set to allow minimal time for the pendulum to reach the inverted pendulum region. For simplicity, the set of gains for the controller in this region is determined through trial and error of the simulated model in MATLAB, and is given by:

$$K_p = 1.0, \quad T_i = 0.1, \quad T_d = 20 \tag{21}$$

The implementation of the PID gains of Equation (21) onto the apparatus of Figure 1 is now done through the PLC command `PID(88)`. Figure 6 shows the responses from the PLC datalogger, where the set point (green) is fixed at 46° to ensure that the pendulum now reaches the inverted pendulum region. The red signal denotes the control response of the pendulum. Datalogging begins at $t = 0.8$ s, and ends when the system finally reaches the inverted pendulum region at $t = 4.7$ s. This means that the system achieves the inverted pendulum region in $t = 3.9$ s.

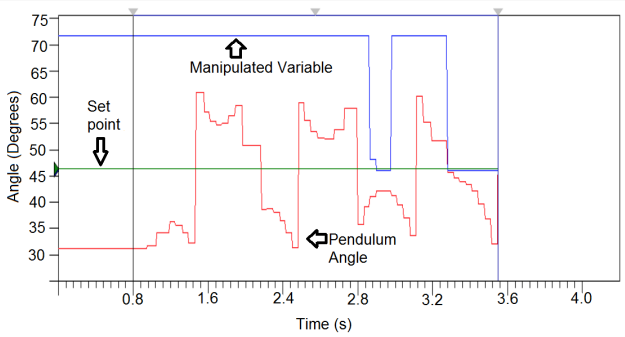

Fig. 6. The control responses from implementing Equation (21) onto the apparatus of Figure 1.

E. Controlling the inverted pendulum in the inverted region

As discussed in Section III-C, the inverted pendulum region is one where linear model approximations can be sufficiently made to the dynamics of the pendulum. In this light, designing a simple PID controller whose gains are optimally tuned can be done in conjunction with another controller architecture such as LQR. Since PID controllers concerns with the error $e(t)$, such function and their associated derivatives $\dot{e}$ and $\ddot{e}$ have to be defined as states to enable the use of LQR. In this respect, denote the position error as e_x, the angular error e_θ, where the relationships between these errors and their desired set point values x_d and θ_d are defined:

$$e_x = x_d - x \tag{22}$$

$$e_\theta = \theta_d - \theta \tag{23}$$

ISBN: 978-988-14047-8-7
ISSN: 2078-0958 (Print); ISSN: 2078-0966 (Online)

Substituting Equations (22) and (23) into the linearized differential Equations (18) and (19) and simplifying yields:

$$\ddot{e}_x = -a_1 e_\theta - a_2 \dot{e}_x - a_3 V \tag{24}$$
$$\ddot{e}_\theta = a_4 e_\theta - a_5 \dot{e}_x + a_6 V \tag{25}$$

where:

$$a_1 = -\frac{mg}{M}, \quad a_2 = \frac{\gamma_2}{M}, \quad a_3 = \frac{\gamma_1}{M} \tag{26a}$$
$$a_4 = \frac{(M+m)g}{ml}, \quad a_5 = \frac{\gamma_2}{Ml}, \quad a_6 = \frac{\gamma_1}{Ml} \tag{26b}$$

where the physical parameters are given in Table I.

TABLE I
THE PHYSICAL PARAMETERS OF THE INVERTED PENDULUM SYSTEM.

Physical Description	Pendulum	Cart	Support
Length	250 mm	300 mm	500 mm
Mass	156 g	450 g	–

The states x_1 to x_5 for this system are now defined:

$$x_1 = e_x, \quad x_2 = \dot{e}_x, \quad x_3 = \int_0^t e_\theta \, dt \tag{27}$$
$$x_4 = e_\theta, \quad x_5 = \dot{e}_\theta. \tag{28}$$

The absence of the term $\int_0^t e_x \, dt$ is due to the fact that the control is primarily concerned with stabilization of the inverted pendulum at the upright position without regard to its position errors. Equations (24) and (25) can therefore be written as a state space system with the following state matrices:

$$\mathbf{A}_\theta = \begin{bmatrix} 0 & 1 & 0 & 0 & 0 \\ 0 & -a_2 & 0 & a_1 & 0 \\ 0 & 0 & 0 & 1 & 0 \\ 0 & 0 & 0 & 0 & 1 \\ 0 & -a_5 & 0 & a_4 & 0 \end{bmatrix}, \ \mathbf{B}_\theta = \begin{bmatrix} 0, -a_3, 0, 0, a_6 \end{bmatrix}^T \tag{29}$$

Although the inverted pendulum region was defined to lie within the angles of 45° < θ < -45°, as depicted in Figure 4, some nonlinearities may still exist around the edge of the region, particularly during the transition from the normal pendulum region to the inverted pendulum region. In order to keep the controller design simple whilst coping with these nonlinearities, the overshoot is allowed to be quite large ($\approx$ 90%). The settling time is designed to be 3 s. The damping factor ζ and natural frequency ω_n are related to the settling time T_s and the percentage overshoot %OS by [10]:

$$\zeta = \frac{-\ln(\%\text{OS}/100)}{\sqrt{\pi^2 + \ln^2(\%\text{OS}/100)}} \tag{30}$$
$$\omega_n = \frac{-\ln(0.02\sqrt{1-\zeta^2}}{\zeta T_s}. \tag{31}$$

Substituting %OS = 90 and $T_s = 3$ into Equations (30) and (31) yields:

$$\zeta = 0.5 \quad \omega_n = 4 \tag{32}$$

To compute the LQR gains using the algebraic method of Section 2.2, first the parameter r is arbitrarily chosen to be $r = 0.1$. The parameters p_{12}, p_{13}, p_{15}, p_{24}, p_{25}, p_{45} and p_{55} are then chosen as follows:

$$p_{12} = 0.2, p_{13} = 0.25, \ p_{15} = 0.25,$$
$$p_{24} = 0.25, p_{45} = 0.3 p_{55} = 0.25 \tag{33}$$

Substituting the parameters of Equations (32) and (33), along with the parameters in Table I, into Equations (13a) - (13c), (15a) - (15e) and (16) yields:

$$\mathbf{K}_{\text{design}} = \begin{bmatrix} 1, 1, 1, 3, 6 \end{bmatrix}^T \tag{34}$$

The last three elements of matrix $\mathbf{K}$ are the proportional gain K_p, the integral gain K_I and the derivative gain K_D of the conventional PID controller. The PLC version of the PID controller, however, slightly modifies the conventional PID controller where K_i and K_d are defined in terms of the integral time T_i and derivative time T_d [11]:

$$K_i = \frac{K_p}{T_i}, \quad K_d = K_p T_d \tag{35}$$

The set of gains in vector $\mathbf{K}_{\text{design}}$ is first simulated via the `lqr` command in MATLAB. Figure 7 plots the simulated e_θ response. It is evident here that the maximum overshoot of e_θ at 90% occurs around 0.5 s, then reaches the steady state at around 3.0 s as designed.

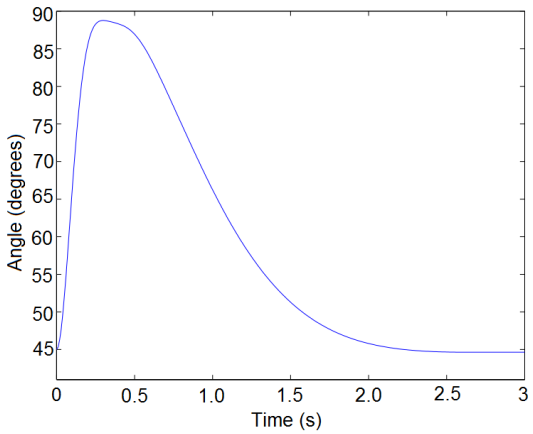

Fig. 7. The simulated control response with $\mathbf{K}_{\text{design}}$ of Equation (34)

Vector $\mathbf{K}_{\text{design}}$ in its present form is suitable only for simulation on a computer aided design software such as MATLAB or Simulink. In order to implement the gains of Equation (34) on to the inverted pendulum apparatus of Figure 1, the last three elements of $\mathbf{K}_{\text{design}}$ need to be converted to the PLC version of the PID controller. Substituting the last three element of vector $\mathbf{K}_{\text{design}}$ into Equation (35) and solving for the integral time T_i and derivative time T_d yields:

$$K_p = 3, \quad T_i = 1, \quad T_d = 2 \tag{36}$$

The gains of Equation (36) is now implemented onto the inverted pendulum apparatus of Figure 1 through the command `PID(88)` as was done for the pendulum region. Figure **??** plots the response from the PLC datalogger. It is evident from this figure that there are some significant overshoots of around 70% around the 0° setpoint. Such overshoot is likely due to the fact that the pendulum itself is operating around the edges of the inverted pendulum region, where the nonlinearities were still prevalent. However the pendulum finally

ISBN: 978-988-14047-8-7
ISSN: 2078-0958 (Print); ISSN: 2078-0966 (Online)

reaches 0° at around 3 s as designed. This was also expected since the controller designs already allowed the overshoot to be up to 90% to cater for the nonlinearity effects. These results show that having an allowable margin of errors could prove to be a useful approach in controller designs when there exists some unmodelled effects. This concept is already prevalent in many other engineering disciplines such as civil engineering.

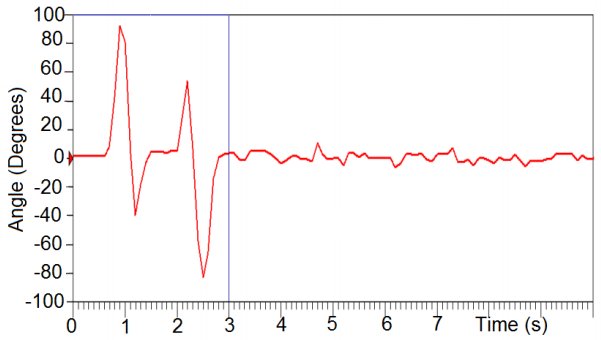

Fig. 8. The angle error responses from implementing the controller of Equation (36) onto the apparatus of Figure 1.

To further test the set of gains of Equation (36) on the inverted pendulum apparatus, four other sets of gains are set as a comparison:

$$G_1 = \{K_p = 1, \quad T_i = 1, \quad T_d = 1\} \tag{37a}$$
$$G_2 = \{K_p = 1, \quad T_i = 1, \quad T_d = 2\} \tag{37b}$$
$$G_3 = \{K_p = 1, \quad T_i = 2, \quad T_d = 1\} \tag{37c}$$
$$G_4 = \{K_p = 2, \quad T_i = 1, \quad T_d = 2\} \tag{37d}$$

Each set of gains of Equations (36), (37a) - (37d) are implemented onto the inverted pendulum apparatus 8 times. For each of the trials, three possible scores based on the experimental stability of the controlled responses is noted. The trial is denoted "S" if the pendulum stays on the upright position without any vibration, in other words, the system is stable; "MS" if the pendulum vibrates while at the upright position, or in other words, being marginally stable, and "US" if the pendulum system is completely unstable, that is, does not stay on the upright position at all. Table II shows the experimental stability results.

TABLE II
THE EXPERIMENTAL STABILITY RESULTS OF THE PLC-BASED INVERTED PENDULUM DESIGNS FOR THE SET OF GAINS OF EQUATIONS (36), (37A) - (37D).

Gains/Trial	1	2	3	4	5	6	7	8
{1,1,1}	S	US	S	US	S	US	US	US
{1,1,2}	S	MS	S	S	US	US	US	S
{1,2,1}	S	US	US	US	S	US	US	S
{2,1,2}	US	S	US	S	S	US	MS	S
{3,1,2}	S	S	MS	S	S	MS	S	S

It is seen from Table I that the designed set of gains of {3,1,2} results in the most stable pendulum system with 100% of the controlled responses being either completely stable or marginally stable. This result validates that the designed set of gains is capable of handling the nonlinearities that were still prevalent around the edges of the inverted pendulum region.

IV. CONCLUSION

This work has presented an LQR based PID controller to control the inverted pendulum system. To facilitate an integration with a PLC, the control design uses a control zoning approach where the entire pendulum is divided into two regions: a normal pendulum regions where the nonlinearities are inherent, and the inverted pendulum region where the system is approximately linear close to the upright position. The errors in position and angle are denoted control states to enable the use of the LQR architecture to obtain the optimal gains for the PID controller. An algebraic approach was also presented to allow a systematic method for selection of the $\mathbf{Q}$ and $\mathbf{R}$ matrices, which in turn yielded an optimal set of control gains $\mathbf{K}_{\text{design}}$. Experimental implementations with the PLC based system show that the computed gains yield the most stable controlled responses compared to the gains chosen through trial and errors, which would be the case with implementations onto the real world system.

There are many other controller designs in the literature for the inverted pendulum system. However these methods typically make very strong assumptions on the validity of the system model. Although these controller designs share the flexibility of being tunable online to compensate for modelling errors, they typically require large amount of computational efforts. The approach in this paper uses the control zoning to effectively set an allowable margin of errors in face of unmodelled effects. This approach alleviates the computational loadings and simplify implementations. In any practical system the simpler the controller design the less chance of coding errors and hardware failures.

REFERENCES

[1] C. Knospe, "PID control", *IEEE Control Systems Magazine*, Vol. 26, pp. 30-31, 2006.
[2] D.H. Kim and J.H. Cho,"Intelligent tuning of PID controller with disturbance function using immune algorithm," *Proc. of the IEEE Annual Meeting Fuzzy Information Processing*, pp. 286-291, 2004.
[3] M. I. Solihin *et al.*, "Optimal PID controller tuning of automatic gantry crane using PSO algorithm", *Proc. of the 5th International Symposium on Mechatronics and its Applications*, pp. 1-5, 2008.
[4] H. Paganagopoulos *et al.*, "Optimal tuning of PID controllers for first order plus time delay models using dimensional analysis". *IEE Proceedings*, Vol. 149, no.1, pp. 32-40, 2002.
[5] C. Hwang and C. Y. Hsiao, "Solution of a non-convex optimization arising in PI/PID control design," *Automatica*, Vol. 38, no.11, pp. 1895-1904, 2002.
[6] G. Ray *et al.*, "Stabilization of inverted pendulum via fuzzy control". *Journal of the institution of engineers (India) Electrical Engineering*, Vol. 88, pp. 58-62, 2007.
[7] Y. M. Liu *et al.*, "Real-time controlling of inverted pendulum by fuzzy logic". *Proc. of IEEE International Conference on Automation and Logistics*, pp. 1180-1183, 2009.
[8] A.E. Bryson Jr. and Y. C. Ho, "Applied Optimal Control", USA. 1975.
[9] E. V. Kumar, J. Jerome, and K. Srikanth, "Algebraic approach for selecting the weighting matrices of linear quadratic regulator", *Proc. of the International Conference on Green Computing Communication and Electrical Engineering*, pp. 1-6, 2014.
[10] G. F. Franklin, J. Da Powell, A. Emani-Naeini, *Feedback Control of Dynamic Systems, 7th Ed.* Pearson, 2015
[11] D. Seborg and T. Edgar, *Process Dynamics and Control, 3rd Ed.*, Wiley, 2010

ISBN: 978-988-14047-8-7
ISSN: 2078-0958 (Print); ISSN: 2078-0966 (Online)